Gadobenate Dimeglumine as an Intrabiliary Contrast Agent: Comparison with Mangafodipir Trisodium with Respect to Non-dilated Biliary Tree Depiction

Joon Seok Lim, MD[1]
Myeong-Jin Kim, MD[1,2,3]
Yong Yun Jung, MD[1]
Ki Whang Kim, MD[1]

Objective: To compare the efficacy of Mangafodipir trisodium (Mn-DPDP)-enhanced MR cholangiogrphy (MRC) and Gadobenate dimeglumine (Gd-BOPTA)-enhanced MRC in visualizing a non-dilated biliary system.

Materials and Methods: Eighty-eight healthy liver donor candidates underwent contrast-enhanced T1-weighted MRC. Mn-DPDP and Gd-BOPTA was used in 36 and 52 patients, respectively. Two radiologists reviewed the MR images and rated the visualization of the common duct, the right and left hepatic ducts, and the second-order branches using a 4-point scale. The contrast-to-noise ratio (CNR) of the common duct to the liver in the two groups was also compared.

Results: Mn-DPDP MRC and Gd-BOPTA MRC both showed similar visualization grades in the common duct (p = .380, Mann-Whitney U test). In the case of the proximal bile ducts, the median visualization grade was significantly higher with Gd-BOPTA MRC than with Mn-DPDP MRC (right hepatic duct: p = 0.016, left hepatic duct: p = 0.014, right secondary order branches: p = 0.006, left secondary order branches, p = 0.003). The common duct-to-liver CNR of the Gd-BOPTA MRC group was significantly higher (38.90 ±24.50) than that of the Mn-DPDP MRC group (24.14 ±17.98) (p = .003, Student's t test).

Conclusion: Gd-BOPTA, as a biliary contrast agent, is a potential substitute for Mn-DPDP.

Index terms:
Magnetic resonance (MR), contrast media
Bile duct radiography, technology
Bile ducts, anatomy

Korean J Radiol 2005;6:229-234
Received May 25, 2005; accepted after revision July 21, 2005.

Department of [1]Diagnostic Radiology, [2]Brain Korea 21 Project of Medical Science, [3]Institute of Gastroenterology, Yonsei University College of Medicine, Korea

Address reprint requests to:
Myeong-Jin Kim, MD, Department of Diagnostic Radiology, Yonsei University Medical College, 134 Shinchon-dong, Seodaemoon-gu, Seoul 120-752, Korea.
Tel. (822) 228-7401
Fax. (822) 393-3035
e-mail: kimnex@yumc.yonsei.ac.kr

Current state of the art MR cholangiographic examination, which relies upon the T2-weighted sequences, is highly accurate in identifying biliary diseases (1−3). However, the T2-weighted MR cholangiography (MRC) has diagnostic limitations which include poor visualization of the intrahepatic biliary tree compared with the extrahepatic biliary tree (4, 5), variation in the degree of T2-weighting that might obscure the biliary structures (6), and limited spatial resolution.

During the past few years, T1-weighted MRC using hepatocyte-directed contrast agents has created interest in the field of MRC because of its potential to provide functional information and to improve the visualization of the non-dilated biliary system (7−13). Initially, mangafodipir trisodium (Mn-DPDP), which is mainly being excreted into biliary system, has been used for this purpose (8, 9, 11−13). However, dynamic MR imaging of the liver cannot be performed because this agent needs to be administered slowly. Recently, contrast agents that are excreted through both the renal and biliary pathways, such as gadobenate dimeglumine (Gd-BOPTA) have become available (14−17). Using a bolus injection technique, these agents can be used for dynamic imaging as an extracellular space agent in the early phase as well as a biliary contrast agent in the delayed phase. However, because the proportion of the amount that is excreted through the biliary system is relatively small, the scan window

for the biliary imaging should be delayed more compared to manganese agents. To our knowledge, the relative efficacy of these two agents in terms of ductal visualization has not been compared directly.

The aim of this study was to investigate the feasibility of Gd-BOPTA MRC and to compare it with Mn-DPDP MRC in terms of the extrahepatic and intrahepatic ductal visualization in patients with a normal or undilated biliary system.

MATERIALS AND METHODS

Eighty-eight healthy liver donor candidates underwent contrast enhanced T1-weighted MRC. Between April 2001 and June 2003, liver donor candidates (age range, 19–54 years; mean age, 34.1 years) (21 women and 67 men) underwent an evaluation with MR imaging. Mn-DPDP was used as an intrabiliary T1 contrast agent in 36 patients between April 2001 and April 2002, and Gd-BOPTA was used in 52 patients between May 2002 and June 2003. None of the subjects had known or suspected biliary abnormalities at the time of the examination. Our institutional review board approved all aspects of this retrospective study and did not require informed consent from any patients whose records were included in our study.

MR Imaging Technique

Both Mn-DPDP MRC and Gd-BOPTA MRC examinations were performed with a 1.5-T imaging system, using a torso phased array coil at one of the two MR systems. (Horizon, GE Medical Systems, Milwaukee, WI; Philips Medical Systems, Best, the Netherlands). Thirty five Mn-DPDP MRC examinations were performed using the former and one Mn-DPDP MRC examination and all Gd-BOPTA MRC examinations were performed using the latter.

Mn-DPDP MRC was obtained following an IV injection of mangafodipir trisodium (Teslascan; Nycomed, Princeton, NJ) at the standard dose of 5 μmol/kg (0.5 mL/kg) administered via a slow injection for 1–2 min followed by a 10-mL saline flush. Fifteen to 30 min after the injection, axial and coronal volumetric 3D spoiled gradient-echo acquisitions of the liver and biliary system were performed, using the following parameters: TR range/TE, 5–8/minimum; flip angle, 20°; matrix, 256 × 160; field of view, 34 cm using a rectangular field of view; and 4 mm slice thickness with a 2-mm reconstruction interval. In the case of Gd-BOPTA MRC, three-dimensional (3D) breath-hold T1-weighted fast-field-echo acquisitions were performed 60–90 minutes after the intravenous administration of the Gd-BOPTA (Multihance, Bracco, Milan) at a dose of 0.2 mmol/kg of body weight. The contrast agent was infused using an automated injector for 12 seconds at a volume-adjusted rate ranging between 2.5 and 3.5 mL/s. The axial and coronal images were obtained using the following parameters: TR range/TE, 5.1/1.47; flip angle, 40°; matrix, 512 × 160; field of view, 34 cm using a rectangular field of view; and a 2 mm slice thickness with a 1-mm reconstruction interval.

Qualitative and Semiquantitative Image Analysis

Two experienced gastrointestinal radiologists analyzed the images retrospectively. They independently reviewed the Mn-DPDP MRC images and Gd-BOPTA MRC images randomly. Each observer recorded visualization grades of the biliary tree, based on a four-point confidence rating scale, with one representing no visualization and four representing excellent visualization. The following structures were evaluated: the common duct, the right and left hepatic ducts, and the right and left second-order division of the intrahepatic ductal branches. For the semiquantitative analysis, one radiologist performed the operator-defined region-of-interest (ROI) measurements of the mean signal intensity of the common duct, the hepatic parenchyma, and the background noise on the coronal 3D spoiled gradient-echo image of the Mn-DPDP MRC images and Gd-BOPTA-MRC images, using a local picture archiving and communication system (PACS) monitor and Digital Imaging and Communications in Medicine (DICOM) image viewing software π-view version 4.0.1.1; Mediface, Seoul). In order to measure the common duct signal intensity, either circular or ovoid ROIs were drawn to encompass as much of the common duct as possible. For the hepatic parenchyma, the ROIs were set in the area that is devoid of focal changes in signal intensity, large vessels, and prominent artifacts at the same level. The noise was measured on each image using the ROIs positioned just lateral to the abdominal wall. The areas with the most prominent ghost artifacts were not included. The signal-to-noise ratio (SNR) of the common duct and liver was calculated by $SI_{common\ duct}/N_{sd}$ and SI_{liver}/N_{sd}, respectively, where the SIcommon duct and SIliver are the signal intensities of the common duct and the liver, respectively, and the Nsd is the standard deviation of the noise. The contrast-to-noise ratio (CNR) between common duct and liver was calculated by $(SI_{common\ duct} - SI_{liver})/N_{sd}$.

Statistical Analysis

The Mann-Whitney *U* test was used to compare the subjective ratings of the visualization of each segment of the biliary tree between the Mn-DPDP and Gd-BOPTA MRC groups. The mean of the visualization grades for the

two reviewers in each segment was used as a single score. The weighted kappa (κ) test was used to measure the interobserver agreement in the ductal visualization. The degrees of agreement were categorized as follows: κ value of 0.00 –0.20, poor agreement; κ of 0.21 –0.40, fair agreement; κ of 0.41 –0.60, moderate agreement; κ of 0.61 –0.80, good agreement; and κ of 0.81 –1.00, excellent agreement. The student's t test was used to examine the statistical significance in the differences between the SNRs and CNRs of the two methods. A p value < 0.05 was considered statistically significant.

Table 1. Median Visualization Grades According to the Qualitative Analysis

Structure	Mn-DPDP MRC	Gd-BOPTA MRC
Common duct	4.0	4.0
Right hepatic duct*	3.5	4.0
Left hepatic duct*	4.0	4.0
Right second-order bile ducts*	2.5	3.0
Left second-order bile ducts*	2.0	2.8

Note.—*Statistically significant (p < 0.05)

RESULTS

The median visualization grades for the qualitative analysis are shown in Table 1. Mn-DPDP MRC and Gd-BOPTA MRC groups both showed similar visualization grades in the common duct (p = .380, Mann-Whitney U test). In the case of the proximal bile ducts, the median visualization grade was significantly higher in the Gd-BOPTA MRC group than in the Mn-DPDP MRC group (right hepatic duct: p = 0.016, left hepatic duct: p = 0.014, right secondary order branches: p = 0.006, left secondary order branches, p = 0.003) (Figs. 1, 2). The reviewers' agreement for the degree of ductal visualization was fair to moderate (Table 2).

Semiquantitative analysis showed that the mean SNR of the common duct and the liver were 69.92 ±32.34 and 45.78 ±19.57 for Mn-DPDP MRC, 93.65 ±34.00 and 54.75 ±21.83 for Gd-BOPTA MRC, respectively. The mean common duct-to-liver CNR was 24.14 ±17.98 for

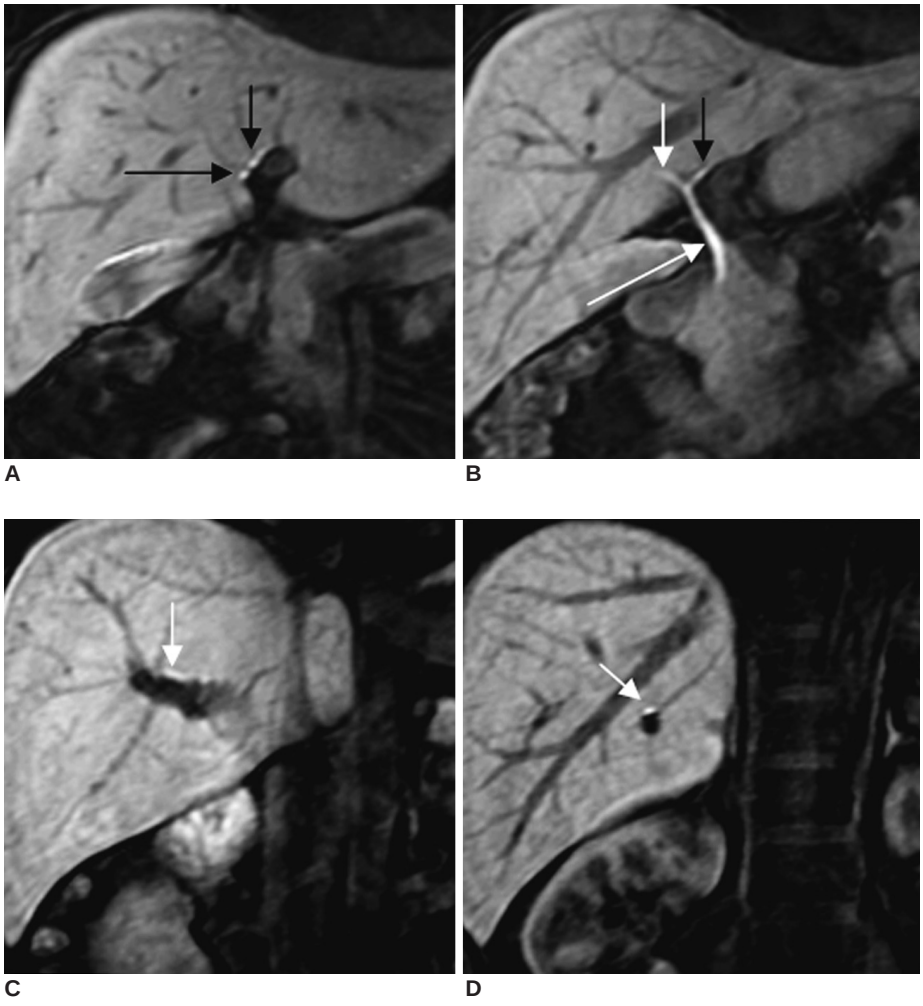

Fig. 1. Mn-DPDP MRC serial images from the anterior to posterior (**A**→**D**) (TR/TE, 5.1/1.47; flip angle, 20°; 4 mm slice thickness) shows a left lateral and medial segment duct (short black arrow and long black arrow in **A**), right and left hepatic duct (short white arrow and black arrow in **B**), common duct (long white arrow in **B**), right anterior segmental duct (white arrow in **C**) and right posterior segmental duct (white arrow in **D**).

the Mn-DPDP MRC group and 38.90 ±24.50 for the Gd-BOPTA MRC group. The mean SNR of the common duct and the common duct-to-liver CNR were significantly higher in the Gd-BOPTA MRC group than in the Mn-DPDP MRC group (p = .002 and p = .003, respectively, Student's t test).

DISCUSSION

Mn-DPDP is the first clinically available hepatocyte-directed agent that is mostly eliminated through the biliary system and enhances the liver signal intensity on T1-weighted images (18−20). Approximately 50−60% of the injected dose was found in the feces, and approximately 15−20% was found in the urine (21). Several reports have confirmed its efficacy as a biliary contrast agent (8, 9, 11, 13). Recently, Lee et al. and Kapoor et al. (9, 11) suggested that Mn-DPDP MRC may facilitate the definition of the intrahepatic bile duct anatomy in healthy liver transplant donor candidates. However, this agent cannot be used for dynamic imaging, which is important in evaluating the vascular anatomy and characterizing focal hepatic lesions.

Gd-BOPTA can be used as a conventional extracellular agent for dynamic MR imaging as well as a hepatocyte-directed agent producing a prolonged enhancement of the liver. A pharmacokinetic study showed that approximately 2−4% of the injected dose is taken up into the functioning hepatocytes and is eliminated through the biliary system (17). Because of this property, Gd-BOPTA has the potential to be a biliary contrast agent. However, to the best of our knowledge, the clinical utility of Gd-BOPTA as a biliary contrast agent has not been evaluated.

Table 2. Inter-observer Agreement According to Kappa Analysis

Structure	Mn-DPDP MRC	Gd-BOPTA MRC
Common duct	0.550	0.658
Right hepatic duct	0.431	0.252
Left hepatic duct	0.293	0.404
Right second-order bile ducts	0.393	0.425
Left second-order bile ducts	0.349	0.242

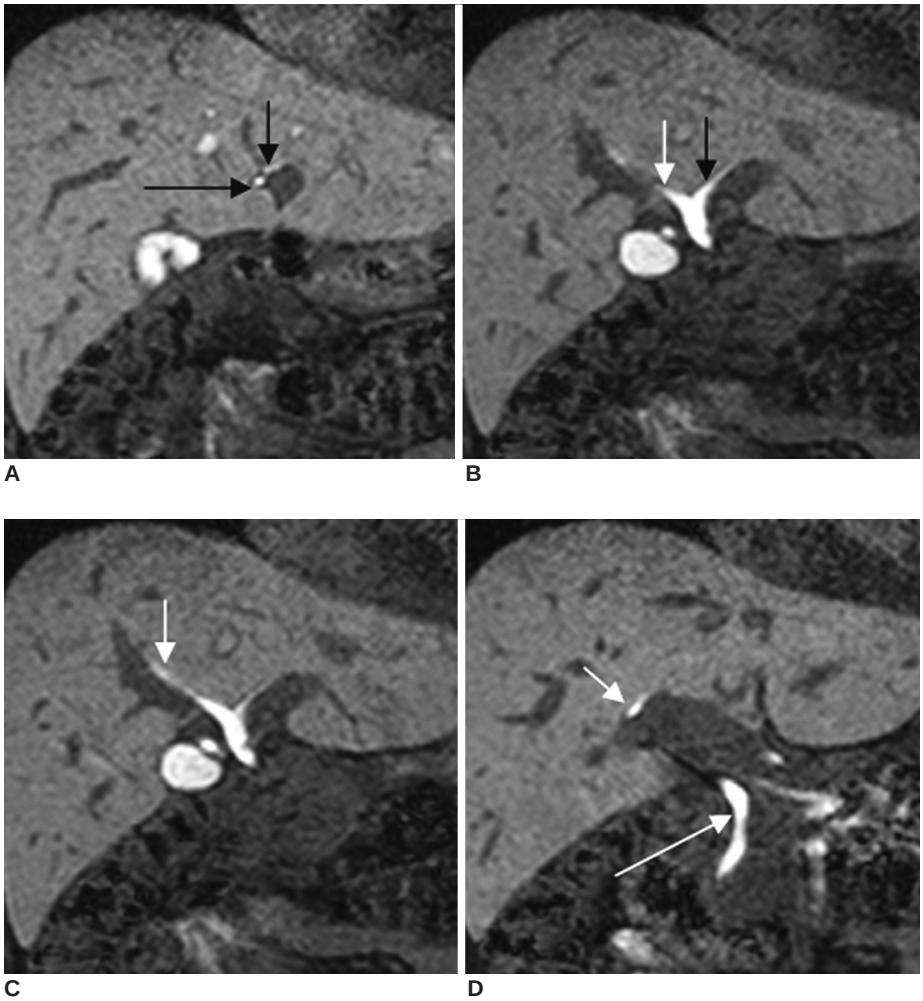

Fig. 2. Gd-BOPTA MRC serial images from the anterior to posterior (A→D) (TR/TE, 5.1/1.47; flip angle, 40°; 2 mm slice thickness) shows a left lateral and medial segment duct (short black arrow and long black arrow in **A**), right and left hepatic duct (white arrow and black arrow in **B**), right anterior segmental duct (white arrow in **C**), right posterior segmental duct (short white arrow in **D**) and common duct (long white arrow in **D**).

This study showed that Gd-BOPTA MRC could be used for anatomic assessments of non-dilated biliary trees and was comparable or superior to Mn-DPDP in terms of the ductal visualization. This is an intriguing result because the proportion of Gd-BOPTA excreted into the biliary system is substantially lower than Mn-DPDP (21). The relaxivity of Gd-BOPTA is higher than that of Mn-DPDP in liver tissue (30 vs. 21.7 [$mmol^{-1}$ S^{-1}]) (22). Macromolecular binding, with the resultant increase in relaxivity, may compensate for the lower hepatocellular uptake of Gd-BOPTA compared to that of Mn-DPDP.

There were some limitations to this study. First, because our study was a retrospective study, a direct comparison of both contrast agents in the same patient was not performed. In addition, the depiction of the biliary tree on the contrast enhanced MRC may show a different result based on the liver function regardless of the administered contrast agents. However, this study included only healthy liver donor candidates with normal functioning livers. Second, the Mn-DPDP-enhanced and the Gd-BOPTA-enhanced MRC were obtained approximately between 15 minutes to 30 minutes, and between 60 minutes to 90 minutes, respectively, after injecting the contrast media. Since we did not obtain serial images from both the Mn-DPDP and Gd-BOPTA MRC, we are not sure whether the delayed images provided best scan window for the biliary tree depiction. However, it was reported that the optimal window for evaluating the liver parenchyma and the bile duct after injection, range from 15 to 20 minutes for Mn-DPDP MRC (7, 9, 13) and 60 to 120 minutes for Gd-BOPTA MRC (23). Third, the MR scanners and the pulse sequence parameters were not the same in the two different contrast-enhanced techniques. Most of the Gd-BOPTA-enhanced MRC was performed using a newer version of the MR system which uses a thinner section thickness. This was because the new MR system was installed during this study. Therefore, the superior results of Gd-BOPTA MRC for intrahepatic duct visualization may be due in part to the more optimized scan parameters. However, our results showed that the Gd-BOPTA-enhanced MRC obtained with updated MR system are comparable to MnDPDP-enhanced MRC obtained by the less updated MR system.

In conclusion, although a fair comparison between the two contrast agents for ductal visualization could not be performed due to the limitations of the study, the data suggest that Gd-BOPTA MRC is comparable to Mn-DPDP MRC in visualizing the biliary duct in either a normal or non-dilated biliary system. Therefore, Gd-BOPTA, as a biliary contrast agent, is a potential substitute for Mn-DPDP.

References

1. Takehara Y. Fast MR imaging for evaluating the pancreaticobiliary system. *Eur J Radiol* 1999;29:211-232
2. Irie H, Honda H, Tajima T, Kuroiwa T, Yoshimitsu K, Makisumi K, et al. Optimal MR cholangiopancreatographic sequence and its clinical application. *Radiology* 1998;206:379-387
3. Fulcher AS, Turner MA, Capps GW, Zfass AM, Baker KM. Half-Fourier RARE MR cholangiopancreatography: experience in 300 subjects. *Radiology* 1998;207:21-32
4. Choi JW, Kim TK, Kim KW, Kim AY, Kim PN, Ha HK, et al. Anatomic variation in intrahepatic bile ducts: an analysis of intraoperative cholangiograms in 300 consecutive donors for living donor liver transplantation. *Korean J Radiol* 2003;4:85-90
5. Hintze RE, Adler A, Veltzke W, Abou-Rebyeh H, Hammerstingl R, Vogl T, et al. Clinical significance of magnetic resonance cholangiopancreatography (MRCP) compared to endoscopic retrograde cholangiopancreatography (ERCP). *Endoscopy* 1997;29:182-187
6. Irie H, Honda H, Kuroiwa T, Yoshimitsu K, Aibe H, Shinozaki K, et al. Pitfalls in MR cholangiopancreatographic interpretation. *Radiographics* 2001;21:23-37
7. Mitchell DG, Alam F. Mangafodipir trisodium: effects on T2- and T1-weighted MR cholangiography. *J Magn Reson Imaging* 1999;9:366-368
8. Papanikolaou N, Prassopoulos P, Eracleous E, Maris T, Gogas C, Gourtsoyiannis N. Contrast-enhanced magnetic resonance cholangiography versus heavily T2-weighted magnetic resonance cholangiography. *Invest Radiol* 2001;36:682-686
9. Lee VS, Rofsky NM, Morgan GR, Teperman LW, Krinsky GA, Berman P, et al. Volumetric mangafodipir trisodium-enhanced cholangiography to define intrahepatic biliary anatomy. *AJR Am J Roentgenol* 2001;176:906-908
10. Carlos RC, Hussain HK, Song JH, Francis IR. Gadolinium-ethoxybenzyl-diethylenetriamine pentaacetic acid as an intrabiliary contrast agent: preliminary assessment. *AJR Am J Roentgenol* 2002;179:87-92
11. Kapoor V, Peterson MS, Baron RL, Patel S, Eghtesad B, Fung JJ. Intrahepatic biliary anatomy of living adult liver donors: correlation of mangafodipir trisodium-enhanced MR cholangiography and intraoperative cholangiography. *AJR Am J Roentgenol* 2002;179:1281-1286
12. Vitellas KM, El-Dieb A, Vaswani KK, Bennett WF, Fromkes J, Ellison C, et al. Using contrast-enhanced MR cholangiography with IV mangafodipir trisodium (Teslascan) to evaluate bile duct leaks after cholecystectomy: a prospective study of 11 patients. *AJR Am J Roentgenol* 2002;179:409-416
13. Kim KW, Park MS, Yu JS, Chung JP, Ryu YH, Lee SI, et al. Acute cholecystitis at T2-weighted and manganese-enhanced T1-weighted MR cholangiography: preliminary study. *Radiology* 2003;227:580-584
14. Marinelli ER, Neubeck R, Song B, Wagler T, Ranganathan RS, Sukumaran K, et al. Synthesis, characterization, and imaging performance of a new class of macrocyclic hepatobiliary MR contrast agents. *Invest Radiol* 2000;35:8-24
15. Kirchin MA, Pirovano GP, Spinazzi A. Gadobenate dimeglumine (Gd-BOPTA). An overview. *Invest Radiol* 1998;33:798-809
16. Lorusso V, Arbughi T, Tirone P, de Haen C. Pharmacokinetics and tissue distribution in animals of gadobenate ion, the magnetic resonance imaging contrast enhancing component of gadobenate dimeglumine 0.5 M solution for injection

(MultiHance). *J Comput Assist Tomogr* 1999;23 Suppl 1:S181-194
17. Spinazzi A, Lorusso V, Pirovano G, Kirchin M. Safety, tolerance, biodistribution, and MR imaging enhancement of the liver with gadobenate dimeglumine: results of clinical pharmacologic and pilot imaging studies in nonpatient and patient volunteers. *Acad Radiol* 1999;6:282-291
18. Elizondo G, Fretz CJ, Stark DD, Rocklage SM, Quay SC, Worah D, et al. Preclinical evaluation of MnDPDP: new paramagnetic hepatobiliary contrast agent for MR imaging. *Radiology* 1991;178:73-78
19. Hamm B, Vogl TJ, Branding G, Schnell B, Taupitz M, Wolf KJ, et al. Focal liver lesions: MR imaging with Mn-DPDP-initial clinical results in 40 patients. *Radiology* 1992;182:167-174
20. Slater GJ, Saini S, Mayo-smith WW, Sharma P, Eisenberg PJ, Hahn PF. Mn-DPDP enhanced MR imaging of the liver: analysis of pulse sequence performance. *Clin Radiol* 1996;51:484-486
21. Wang C, Gordon PB, Hustvedt SO, Grant D, Sterud AT, Martinsen I, et al. MR imaging properties and pharmacokinetics of MnDPDP in healthy volunteers. *Acta Radiol* 1997;38(4 Pt 2):665-676
22. Reimer P, Schneider G, Schima W. Hepatobiliary contrast agents for contrast-enhanced MRI of the liver: properties, clinical development and applications. *Eur Radiol* 2004;14:559-578
23. Caudana R, Morana G, Pirovano GP, Nicoli N, Portuese A, Spinazzi A, et al. Focal malignant hepatic lesions: MR imaging enhanced with gadolinium benzyloxypropionictetra-acetate (BOPTA)-preliminary results of phase II clinical application. *Radiology* 1996;199:513-520